



Data Slicing Processing Method for RE/RP System Based on Spatial Point Cloud Data

Shan Zhong^{1,2}, Yongqiang Yang¹ and Yanlu Huang¹

¹South China University of Technology, <mailto:gotti@cityuny.edu> jonsonzhong@126.com,
meyqyang@scut.edu.cn, yanlu@scut.edu.cn

²Wuzhou University, jonsonzhong@126.com

ABSTRACT

Aiming at the problems of low forming precision and low processing efficiency of the current slicing processing methods using spatial point cloud data for Reverse Engineering/Rapid Prototyping(RE/RP) integrated system, a series of efficient and effective algorithms were proposed. First, the Inverse Distance Square method (IDS) was adopted to determine the direction and thickness to make an adaptive slicing for the spatial point cloud data. Then, the extended extrapolation method was presented to obtain a vertical slicing contour curve. Moreover, the contour points in each layer were searched, sorted and reconstructed by applying Non-Uniform Rational B-spline (NURBS) interpolation method, and the reconstructed profile data points were homogenized and finished. Finally, several simulation results and the practical examples were given to demonstrate the novel methods which have a higher forming precision and processing speed for rapid fabrication.

Keywords: RE/RP, spatial point cloud data, adaptive slicing, reconstructed profile, rapid fabrication.

1. INTRODUCTION

The original data for RE/RP integration system is based on the spatial point cloud from the Reverse Engineering. In the conventional method of data processing for Reverse Engineering/Rapid Prototyping integrated system (RE/RP), it needs collecting the pre-treated (including filtering, and reducing for the data) spatial point cloud data and constructing the triangular mesh based on the straight line which are generated by connecting the points one by one, and then the stereo Lithography interface specification (STL) model is uniformly sliced according to the required precision and the layered contour file is finally obtained. This method has some drawbacks such as the difficulties of reconstructing the triangular mesh with the original points, low reconstructing speed with the huge data of the generated STL file, and low approximation accuracy with the high redundancy which seriously impacts the RP precision in the subsequent processing. So it is important and significant to explore a new method for data slicing processing of the spatial point cloud in the RE/RP system. Direct slicing method using spatial point cloud data can avoid these intermediate procedures such as reconstructing the triangular mesh and generating

the STL file. It not only reduces the complexity and calculation time of the data processing for model reconstruction, but also overcomes the shortcomings of the STL file with large quantity of data and needing reparation [1]. The conventional STL model slicing method and the direct slicing method are compared as shown in Fig. 1. Obviously the method is simpler, and it can improve the speed of data processing.

The whole data processing steps for direct slicing of the spatial point cloud data are as follows: Firstly, the slicing direction and thickness with the spatial point cloud data were determined, and all the contour points in each slice were obtained. Secondly, the contour points in each layer were reconstructed. Thirdly, the reconstructed profile data points were homogenized and finished to fulfill the requirements of the subsequent processing for rapid prototyping.

2. RELATED WORK

At present, there are mainly two methods of slicing with spatial point cloud, as so-called projection method and slicing contour area method. The projection method was adopted to determine the layered thickness by Zhang and Wong [2]. Firstly, a set of

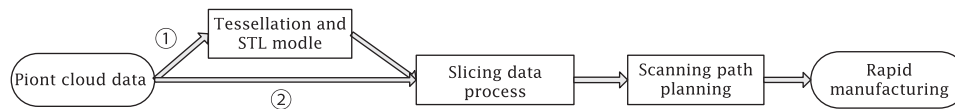


Fig. 1: Comparison of the conventional and the direct slicing methods.

unorganized point cloud was divided into a number of layers by slicing the point cloud along the given building direction. Secondly, the data points were projected onto a plane. These projected data points were sorted to keep only the key feature points using a reduction method based on the linear correlation. The feature points were used to generate a polygon. The maximum allowable deviation of the points in the layer was compared to the given shape error to decide whether to reduce or increase the layer thickness. Then, this process was repeated until the maximum deviation was just below the given shape error. Using this method, all characteristic points of the layered contour were obtained by analyzing the segment linear correlation, and sliced contour polygon was restructured. However, there are some shortcomings such as slow data processing speed and low forming accuracy; Wu [3] proposed an adaptive slicing approach with a minimum number of layers based on given shape error. The local linear relationships among the projection points were defined through calculating the correlation coefficients, so that the orderly layers contour curves were formed, and then the layer thickness was gradually approximated using the recursive method. When the shape error between two layers was less than the specified value the layer thickness was finally obtained. The advantage of this algorithm is that it can directly control the parts surface quality through the specified surface shape error, but the calculation of the shape error is complicated and difficult.

For the adaptive slicing of spatial point cloud in the vertical direction, Lee studied a method using the curvature information extracted from the point cloud [4]. Firstly, the point cloud model was preliminary sliced according to the extracted characteristic points, and the curvature of the point cloud data was obtained from the curve profile in each layer; then the spatial point cloud was divided into different regions based on different curvatures. Secondly, the distance from the point cloud to the contour curve in each region was calculated. An additional layer would be inserted between two layers if this distance went beyond an user-defined threshold. This approach was obviously complex and time-consuming. Meanwhile, a method in which the layer thickness was controlled by the narrow width of the data points on the slicing plane was addressed, and the adaptive slicing was implemented by using the interpolation method in the intermediate layers [5]. The binary image was obtained through the binarization of the projection point cloud, and the radial width of the projective

point cloud in the image was calculated. Then, the maximum width was defined as the radial shape error and was used to decide whether a new layer should be added between the initial ones, so the complete layered contour was obtained. This method did not improve the slicing speed.

After determining the layered thickness, the curve profile would be reconstructed on each layer. Sun et al presented an intersection method to extract the surface contour line at the minimum distance-based correlated point-pairs [6]. He claimed that the sliced contour had relations only with its nearest domains in the point cloud model, which was called as correlated domains. The points closer to the sliced plane would impact the contour reconstruction seriously. These points were named as correlated points while others were named as uncorrelated points. According to this rule, the distance from the point to the sliced plane was calculated and used to judge whether the point was in the correlated domain. The minimum distance-based correlated point-pairs were found in the point set. By computing the intersection of the correlated point pairs and the sliced plane, all data points can be obtained on the sliced contour. Then, these data points were orderly connected and homogenized, and the obtained sliced contour can be directly inputted to the rapid prototyping machines. In addition, Liu et al presented an intermediate point-based curve model (IPCM) [7]. They subdivided the cloud data into a set of domains according to a given subdivision error, and the data in each domain were compressed according to the user-defined shape tolerance. Then an IPCM was constructed based on the feature points of each domain, and RP layer profiles were directly extracted from the models. Finally the RP layer profiles were faired with a discrete curvature and subsequently closed to generate the final layer-based RP model. Levin first applied the moving least-square method on the sliced contour curve reconstruction from scattered point cloud [8]. His main idea was that a weighted average method was used for each data point, and a curve was regressed by using its neighborhood data points. Then the points would be moved to a new position into the fitting curve. Thus the curve profile was reconstructed and the local error of the reconstructed curve was determined by an optimal approximation error of a local polynomial.

Generally speaking, for adaptive slicing method of the spatial point cloud, the projection method is used to determine the sliced thickness according to the average projection shape error between spatial point cloud and the sliced projection plane, and the sliced

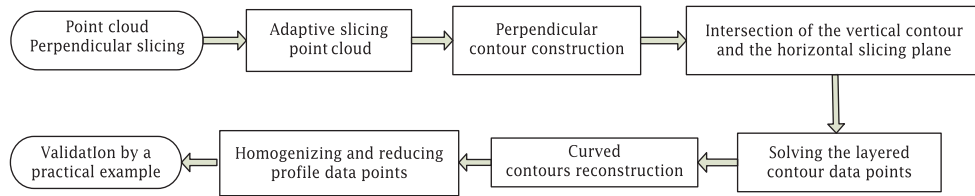


Fig. 2: Flow chart of slicing data in this study.

contour curve is reconstructed by using the projection points which meets the conditions set by some rules. This method can obtain a precise layered contour for the spatial point cloud with a simple surface model and uniform distribution data. When the model is with complex shape and structure, this method is hard to assure the precision because there is no direct relationship between the distance of spatial point cloud to the projection plane and the projection shape error.

The slicing contour area method usually adopts a uniform thickness to slice the spatial point cloud and then calculates the change rate of the areas of the adjacent layers using scan method. The layered thickness would be adjusted according to the above change rate and so the adaptive slicing is realized. This method can achieve a higher accuracy for the scattered spatial point cloud, but the algorithm has lower operating speed because of the area calculation of each layer.

For curved profile reconstruction on each layer, the line and plane intersection method is limited in application because the correlated points and the uncorrelated points are hard to judge, and the sliced contour information is easy to lose; For the method using moving least-square there are disadvantages such as lower fitting precision and lower efficiency using IPCM.

To solve the problems of low accuracy and complicated steps in conventional methods of slicing spatial point cloud data in the RE/RP integrated system, a series of efficient and effective algorithms are proposed in this paper. Our works include the following parts. Firstly, to obtain adaptive slicing thickness of the spatial point cloud, the vertical projection planes should be built and the spatial point cloud should be projected to the vertical planes. Secondly, an adaptive slicing method is implemented by using Inverse Distance Square method (IDS) to obtain the adaptive layer thickness with this projected point cloud. Thirdly, to obtain accurate nodes in sliced contour curves, the point cloud model is sliced vertically, and the extended extrapolation algorithm including searching and sorting the spatial point cloud on the perpendicular projection plane is described in detail, and the extrapolating curve (namely vertical contour curve) is reconstructed. Fourthly, by computing the intersection between the above-mentioned vertical contour and the horizontally sliced plane, all nodes can be worked out on each horizontal slice plane. For generating a

uniformly smooth contour curve on the horizontal slice plane, the NURBS curve interpolation method is adopted to reconstruct the curve profiles of each layer by using these nodes. Finally, considering the adaptability of the data on subsequent computer numerical control (CNC) interpolation, the layer contour data are quantitatively reduced and homogenized. Based on the series of algorithms, the data suitable for RE/RP integrated system are obtained. The presented methods are validated by several simulation results and a practical example using a rapid prototyping machine. The data processing flow chart of the presented methods in this study is shown in Fig. 2.

3. PERPENDICULAR SLICING AND ESTABLISHMENT OF THE VERTICAL PROJECTION FOR SPATIAL POINT CLOUD

To adaptively slice the spatial point cloud, the vertical projection planes should be built firstly. The point cloud which has been measured and pre-processed (including filtering and reducing the data) is sliced vertically.

Suppose the pre-processed 3D point cloud is named as $\Omega = \{d_1, d_2, \dots, d_n\}$, $d_n = \{x_i, y_i, z_i | i = 1, 2, 3 \dots n\}$, and its bounding box is defined as $A = [x_{\min}, x_{\max}] \times [y_{\min}, y_{\max}] \times [z_{\min}, z_{\max}]$. Establishment of the vertical projection plane follows these steps.

Step 1. Determine the vertical slicing direction. The vertical slicing direction is in fact the normal direction of the horizontal slicing plane, so we find the horizontal slicing direction in the spatial point cloud with the following method. First, the quadric surface in the local coordinate system is used to approximate the point cloud, and the curvature, with the essence of differential, is calculated in orthogonal cross section (OCS) [9]. When a model is sliced, if the model is smooth and the curvature in each direction changes little, the slicing result is not sensitive to the slicing direction. Whereas, if the curvature changes along a direction significantly larger than other directions, the spatial point cloud should be sliced perpendicular to the direction of larger curvature variation. Then, set the normal direction of the horizontal slicing direction as z , and the vertical slicing direction is determined.

Step 2. Select the vertical line perpendicular to xoy horizontal plane through Z_{\max} , namely the maximum value of z , as the center line of rotational slicing

in the local coordinate system, and then a series of vertical projection planes $S_i (i = 0, 1, \dots, n, \dots)$ can be created with deviation angle $\theta = 360^\circ/n$, as illustrated in Fig. 3. Here n is determined according to the error threshold of layer curve contour.

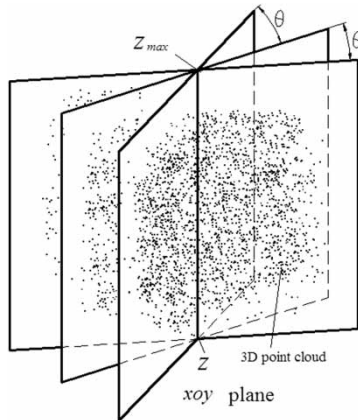


Fig. 3: Sketch of perpendicular projection plane.

Step 3. Project the spatial point cloud to the vertical planes. The vertical plane S_i is converted to S'_i in a two-dimensional coordinate system $y'_i o z'_i$ through rotation and translation. Collect the spatial point cloud with the neighbor distance ε , then project them towards the plane S_i , and the point cloud band $D_i C_i$ is obtained as shown in Fig. 4.

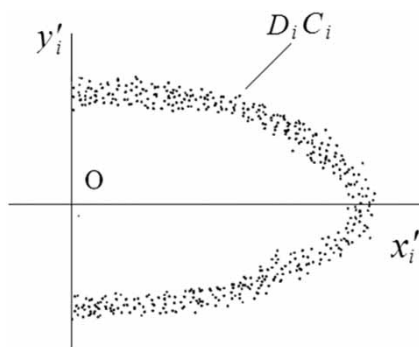


Fig. 4: Cloud band $D_i C_i$ in the first and fourth quadrant of coordinate system $x'_i o y'_i$.

4. ADAPTIVE SLICING OF SPATIAL POINT CLOUD

The precision and speed of data slicing depend on how to determine the appropriate thickness of adaptive slicing with spatial point cloud. Liu et al used the point cloud density as the basis for determining slicing thickness [10]. They predicted the density of the spatial point cloud and set the predicted value as the initial slicing thickness. This kind of calculation was very complicated with high spatial complexity. In addition, the formula contained the uncertainty

empirical coefficient $k = 1 \sim 4$. A method named as IDS was widespread and was used in spatial interpolation of rainfall by Goovaerts [11]. In this method the weight depends on the distance from the sample point to the interpolation point. This method is based on the close similarity principle which means that the closer two objects are the higher similarity they have. In this study the algorithm would be improved to predict the spatial point cloud density, and the predicted value would be taken as slicing thickness.

The slicing thickness for each projection plane is set as δ_{ij} , then the density for the point cloud band $D_i C_i$ on the projection plane S_i of the coordinate system $x'_i o y'_i$ is predicted, and the actual slicing thickness δ_i is calculated with this formula:

$$\delta_i = \frac{\sum_{j=1}^N \delta_{ij}}{N} \quad (4.1)$$

Where N is the number of the projection planes and δ_{ij} can be calculated as follows.

From $x = X_{\min}$, we pick up the points of which the Euclidean distance is less than l for each projection point p_i and then calculate the average distance l_t . Thus we obtain the slicing thickness for each projection as follows.

$$\delta_{ij} = 4.33[x(s_{t+1}) - x(s_t)] = 4.33 \left[\frac{\sum_{t=1}^m y_{t+1}}{l_t^2} / \frac{1}{l_t^2} - \frac{\sum_{t=1}^n y_t}{l_t^2} / \frac{1}{l_t^2} \right] \quad (4.2)$$

Where 4.33 is the empirical value obtained by repeating experiments for spatial point cloud from a laser scanner and processed with the pretreatment. The test point clouds used for experiments are those with smooth surfaces, $x(s_t)$ is the predicted value, and m, n are the used spatial point cloud amount before and after calculation processing, and y_t is the t th point cloud value.

For the point cloud geometry model which contains three features of convex, concave and internal structures, the layer thickness deviation may be caused because of different data cloud densities. The following two ways are used to solve these problems. The first is that the average thickness is taken as layered thickness. The second way is that the three kinds of point cloud bands (convex, concave and internal) are identified, and then the adaptive layer thickness of the three point cloud bands is calculated separately by using IDS method. The minimum value of the three layers thicknesses is taken as the layered thickness. Here the first way is used.

To verify the layered effect, a vase model is used to process the adaptive slicing. Fig. 5 shows the vase point cloud with a total amount of 14689 points.



Fig. 5: Vase model point cloud.

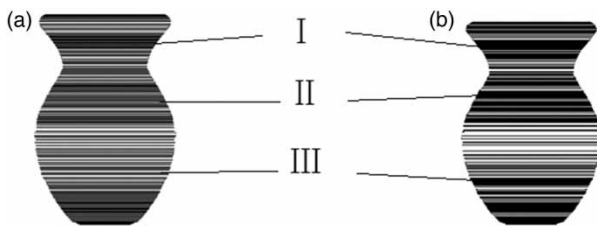


Fig. 6: Results of two adaptive slicing strategies: (a) The general density estimation method, (b) the IDS method.

Slice method	Layers	Layered shape error	Time cost
The general density estimate	181	0.052 mm	57 sec
IDS	130	0.023 mm	33 sec

Tab. 1: The comparison of two kinds of adaptive slicing methods.

Fig. 6(a) shows the adaptive slicing result by using the general density estimation method. Fig. 6(b) presents the adaptive slicing result by using the IDS method. From the part I, II and III of slicing results shown in Fig. 6, the adaptive slicing result is too dense for the general density estimation method. The comparison of two kinds of adaptive slice methods is shown in Table 1. Evidently, IDS method possesses the higher slicing precision because it reduces the redundant slices, and it also improves the layering speed.

5. THE CONTOUR CURVE RECONSTRUCTION ON THE PROJECTION PLANE USING THE VERTICAL SLICING METHOD IN THE SPATIAL POINT CLOUD

After determining the layered thickness using the improved IDS method, all horizontal slices of the point cloud could be obtained, and every contour

curve should be restructured on each horizontally layer. In general, these curves are reconstructed by using the spline interpolation method with the nodes on each layer. Since these points are calculated by the intersection between the vertical curve and horizontal slice in this paper, the vertical contour curve should be determined on the vertical projection plane in advance. Here, the extended extrapolation algorithm of the searching and sorting for spatial point cloud is discussed in detail.

The extrapolation method is the conventional scientific calculation method in engineering applications. To reconstruct the vertical slicing contour curves of the point cloud band on the projection planes, the extrapolation method is adopted. This method uses only a limited priori data, whereas the extrapolation fitting model can apply more prior data not being able to lock the latest data points [12]. The extended extrapolation model inherits the advantages of the least-square method. It obtains better results in the application because the latest data will be used to make interpolation restrictions [13]. However, when the data points are dense, because the latest interpolation point in the original algorithm is only a point, it is easy to cause mutations of the extrapolated curve. Here, the extended extrapolation algorithm will be improved by the following methods.

After the vertical projection planes are built, the data point on the projection planes are searched and sorted by using the improved extended extrapolation algorithm.

Given point cloud data in the increasing chronological order $(x_0, y_0), (x_1, y_1), \dots, (x_i, y_i), \dots, (x_n, y_n), \dots$ ($i = 0, 1, \dots, n, \dots$), the former n points are known. According to the priori data trends, the y_{n+1} value of the next point $x = x_{n+1}$ can be calculated. The extrapolating method is shown in Fig. 7.

Here we note x_n as the latest time, and choose the average of m points of which the Euclidean distance from x_n is less than d as restriction. Because the approximation function may be easy to appear serious oscillation or Runge's phenomenon when using higher order interpolation, the 2nd order approximation is adopted in this paper. The improved extended extrapolation mathematical model is established as below:

$$\begin{cases} \min I(a_1, a_2, a_3) = \sum_{i=1}^n [a_1 + a_2 x_i + a_3 x_i^2 - y_i]^2 \\ \text{s.t.} \quad a_1 + a_2 x_n + a_3 x_n^2 = \frac{1}{m} \left(\sum_{j=n-m+1}^n y_j \right) \end{cases} \quad (5.1)$$

Here a_1, a_2, a_3 are the undetermined coefficients. Solve Eqn. (5.1) and obtain

$$a_1 = \frac{1}{m} \left(\sum_{j=n-m+1}^n y_j \right) - a_2 x_n - a_3 x_n^2 \quad (5.2)$$

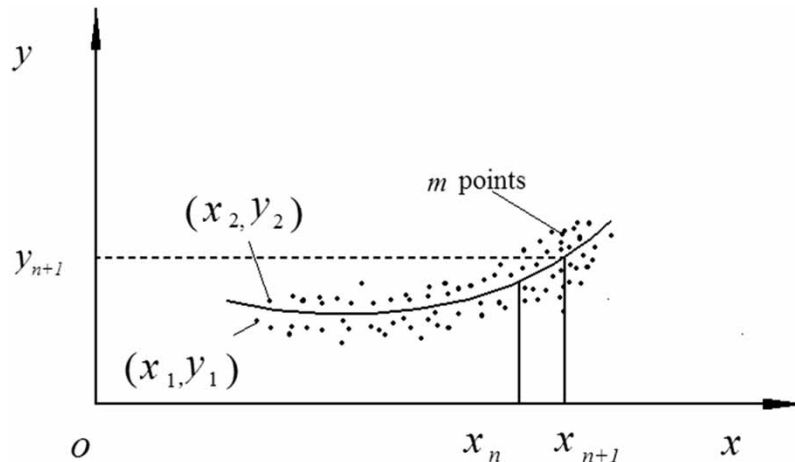


Fig. 7: Data extrapolating sketch.

Substitute Eqn. (5.1) into the Least-square equation.

$$\min I(a_2, a_3) = \sum_{i=1}^n \left[a_3 x_i^2 + a_2 x_i + \frac{1}{m} \left(\sum_{j=n-m+1}^n y_j \right) - y_i - a_2 x_n - a_3 x_n^2 \right]^2 \quad (5.3)$$

Set

$$\begin{cases} \frac{\partial I(a_2, a_3)}{\partial a_2} = 0 \\ \frac{\partial I(a_2, a_3)}{\partial a_3} = 0 \end{cases} \quad (5.4)$$

Solve the above Eqn. (5.3) and Eqn. (5.4) to obtain a_2, a_3 and substitute them into Eqn. (5.2). Thus the a_1 value is obtained.

The extended extrapolation formula is as follows

$$y_k = a_1 + a_2 x_k + a_3 x_k^2, \quad k = n + 1, n + 2 \quad (5.5)$$

For the improved extended extrapolation mathematical model, because the average value of extrapolation points was taken, the solved data were smoother with higher accuracy. The vertical slicing contour curves of the spatial point cloud on the projection planes would be reconstructed by the above extrapolation method.

Considering the designed data is increscent in the extended extrapolation method, $D_i C_i$ band is divided into two parts. One is in the first quadrant and the other is in the fourth quadrant. The profiles of the first quadrant and the fourth quadrant are reconstructed respectively by using the improved extended extrapolation algorithm. Then a curve profile of vertical slices is synthesized as shown in Fig. 4. The nodes on the vertical projection plane are searched and sorted following such steps as below.

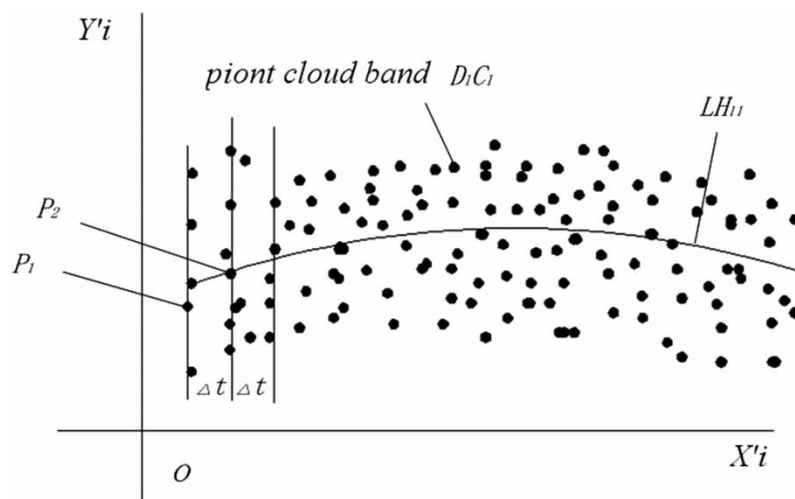


Fig. 8: Solution of extrapolated curve LH_{11} .

Step 1. Determine the initial point of the point cloud on the projection plane. In coordinate system x'_i, y'_i , $P'_1(x'_1, y'_1)$ in the point cloud band $D_i C_i$ is taken as the initial point, where $x'_1 = x'_{\min}$, $y'_1 = \frac{1}{n} \sum_{j=1}^m y_j$. $P'_2(x'_2, y'_2)$ is selected as the second point with equal interval Δx , here $x'_2 = x'_{\min} + \Delta h$, $y'_2 = \frac{1}{2} \sum_{j=1}^n y_j$.

Step 2. Search and determine other extrapolated points in the point cloud band. Use the first point P'_1 and the second point P'_2 as initial data, and adopt the extended extrapolation method described in section 5 to search and determine the third point. It is the one with the shortest distance to the extrapolated curve. Other extrapolated points can be solved with the same approach. The solutions of extrapolated points would be ended until meeting the condition $x' = X'_{\max}$. So, in the first quadrant, an extrapolated curve named LH_{11} is constructed by extrapolated points, as shown in Fig. 8.

Step 3. By the coordinate conversion, we can solve the extrapolated curve (vertical contour curve) named LH_{12} in the fourth quadrant with the above methods, and then construct a successive extrapolated curve named LH_{11} on the S_1 plane synthesized by the curve LH_{11} and LH_{12} . Moreover, all the other extrapolated curves (vertical contour curves) named LH_n can be generated on all of the projection structure surfaces S_i in the same way.

For the point cloud geometry model which contains three features of convex, concave and internal structures, when applying extended extrapolation method to solve an extrapolation curve, three different vertical contour curves can be generated in a certain angle of vertical slicing. Here, they are identified and numbered for classification, and will be used in the next section.

6. SOLVING THE DATA POINTS OF THE HORIZONTALLY SLICED CONTOURS AND RECONSTRUCTING PROFILE CURVES

To reconstruct horizontally sliced contour curves, the adaptive slicing was implemented in the horizontally slicing direction according to the slicing thickness δ_i obtained in the previous section, and so m parallel sliced planes were achieved. These m planes intersect with n curves $LH_i (i = 1, 2, \dots, n)$ which were constructed in the previous method. Thus, the point set with $m \times n$ points of intersection was obtained. Then, by coordinate system conversion, we set $PS_i = \{(x_j, y_j) | j = 1, 2, \dots, n\}$ as the ordered point set on the sliced plane of the i th layer. Because of uneven distribution of the nodes, the non-uniform rational curve interpolation method is used to fit them. NURBS method, comparing with other interpolation methods in the spline curves, can divide and merge in any point with better interpolation performance [14]. The data points inside the point set are put as nodes, and a

smooth layered contour curve can be fitted by using the NURBS method.

Suppose that the k th order NURBS curve is defined by a piecewise rational B-spline basis functions, which is shown as below.

$$p(u) = \frac{\sum_{i=0}^n \omega_i d_i N_{i,k}(u)}{\sum_{i=0}^n \omega_i N_{i,k}(u)} \quad (6.1)$$

Where $\omega_i, i = 0, 1, \dots, n$ is named as weighting factor which is associated with the control vertex $d_i (i = 0, 1, \dots, n)$. The first and last weighting factors are $\omega_0, \omega_n > 0$, and the rest are $\omega_i \geq 0$. $N_{i,k}(u)$ is the k th order standard B-spline basis function determined by the node vector $U = [u_0, u_1, \dots, u_{n+k+1}]$. For the non-periodic NURBS curve, the repeatability of two vertices can be set as $k+1$. In most cases applications, the node values are set to 0 and 1 respectively, and the curve defining domain is set to $u \in [u_k, u_{n+1}] = [0, 1]$. The computing of data parameterization and the inverse calculation refers to the related literature [15].

After obtaining control points, weighting factors and node vectors, the NURBS interpolation curve is determined. The points between the interval $[u_i, u_{i+1}]$ on a slicing plane are interpolated according to the actual requirements, and all node values are calculated by using de Boor algorithm [16]. A golf head model containing the line and spline curve is tested (Fig. 9), and this head model will be sliced by using a vertical projection plane by ninety equal portions (Fig. 10). Further, at $Z = 5.56$ mm, the horizontal layer plane and vertical contour curves intersect, and 90 intersection points are obtained (Fig. 11). Finally, a smooth contour curve is reconstructed after fitting these nodes and interpolating points by using the NURBS method (Fig. 12).

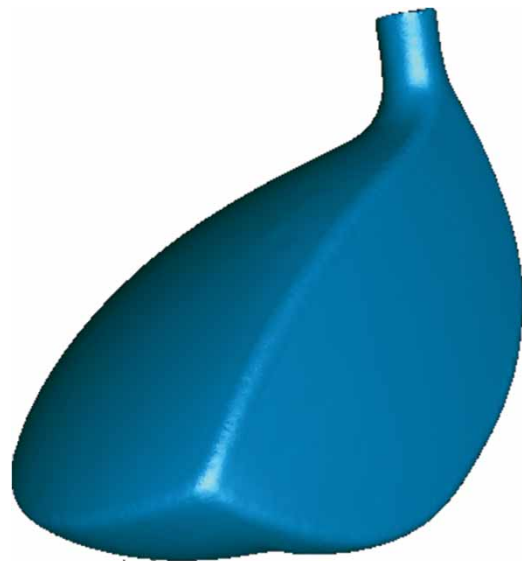


Fig. 9: Golf head model.

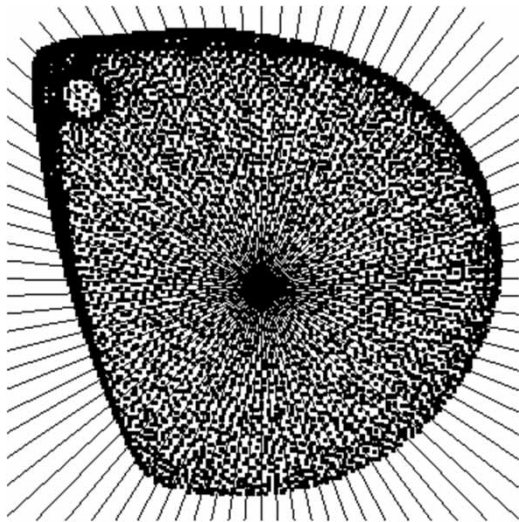


Fig. 10: Golf head model point cloud and vertical projection plane.

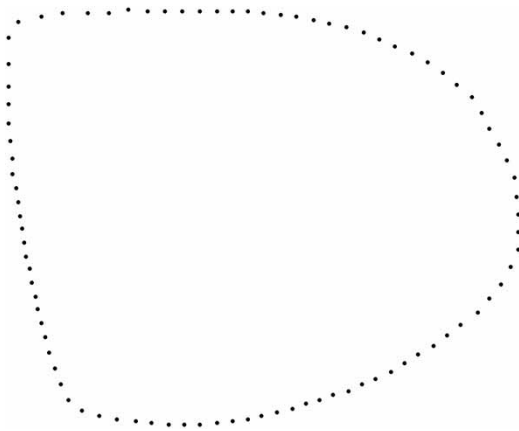


Fig. 11: The intersection points of horizontal plane and vertical contour curves.

If the point cloud geometry model consists of three features of convex, concave and internal structures, three different vertical contour curves can be generated in a certain angle of vertical slicing. These curves will intersect with the horizontal plane. Thus 2*3 nodes (distributed on the left and right sides of a vertical contour curve) may be obtained on each of the horizontal plane in a same vertical slicing angle, which are the intersection points between vertical contour curves and inner loop and outside loop. Here they will be classified and numbered. In this case, because they are still orderly points, the reconstruction of the contour curve in a same horizontal plane is classified into orderly point reconstructions of close inner loop and outer loop. These nodes can also be reconstructed into smooth contour curves by using the NURBS method.

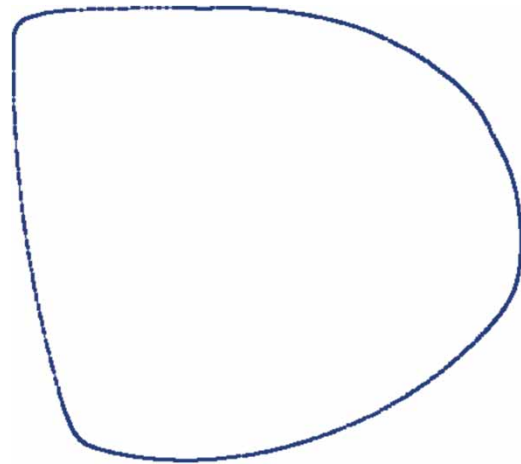


Fig. 12: Contour curve reconstruction of golf head model.

7. HOMOGENIZING AND REDUCING SLICED CONTOUR DATA POINTS

Because there might be redundant points for the NURBS curve composed of nodes and interpolation points, the data feature points should be extracted and their amount should be reduced before processing by the rapid prototyping system. The equal length chord method was adopted to decide retention or deletion of interpolation points [17]. This method easily leads to deletion of useful points. Here, we present the angle error and chord height error method to process NURBS curve profile data, and consider the data points as approximate linear when they are less than the two errors. It not only reduces the sampling points and remains interpolation points at the position with a large curvature change but also ensures the accuracy of global contour curves (Fig. 13).

Suppose that the angle error is $\Delta\alpha$ and the chord height error is Δh , they follow the below formulas:

$$\Delta\alpha = \arcsin \frac{\Delta h}{\sqrt{x^2 + y^2}} \quad (7.1)$$

$$\Delta h = |S(x - x_i) - T(y - y_i)| / \sqrt{S^2 + T^2} \quad (7.2)$$

Where $S = y_{i+1} - y_i$, $T = x_{i+1} - x_i$

In the last section, the curve contours of a golf head model were reconstructed with obtained orderly points using NURBS interpolation method. Now the interpolation points between each interval $[u_i, u_{i+1}]$ are processed. As shown in Fig. 14, there are 158 handled points from the original 271 points. The point amount is greatly reduced by using the angle error and chord height error method.

8. PRACTICAL EXAMPLE

We adopt the presented methods to a rapid fabrication case. The rapid prototyping machine uses

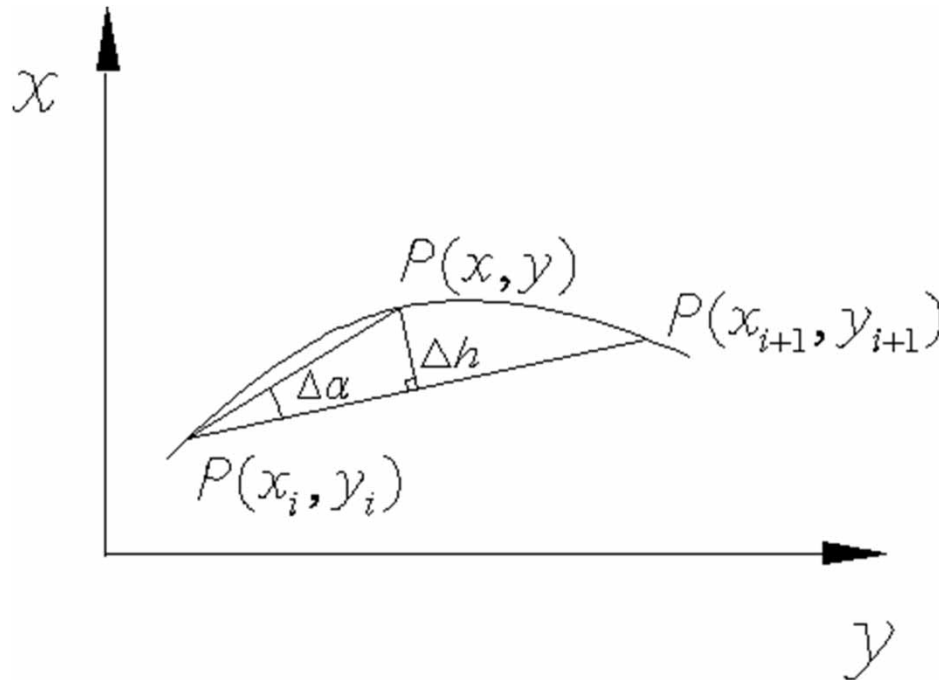


Fig. 13: Sketch of the angle error and chord height error method.

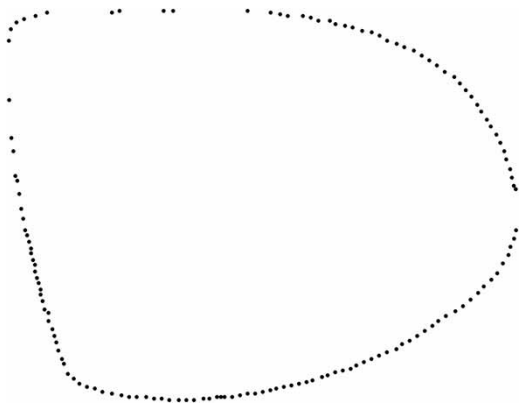


Fig. 14: Reduced golf head model data points.

compound wax as forming materials with the maximum allowable slicing thickness of 0.0127 mm and the highest allowable forming precision of 0.005 mm, and the formed wax model can be applied directly to investment casting. We choose a model composed of complex curved surfaces for spatial point cloud data treating and processing in RE/RP systems and to test the accuracy and speed of data processing using the proposed algorithms.

The shoe model size is $10.15 \times 30.72 \times 16.32 \text{ mm}^3$. And its point cloud is acquired by using the three dimension laser scanning system. There are altogether 5205 points after pre-treating including filtering, reducing and putting together for the data [18] (Fig. 15) and this model has a high forming accuracy requirement. Firstly, we adopt the improved extended

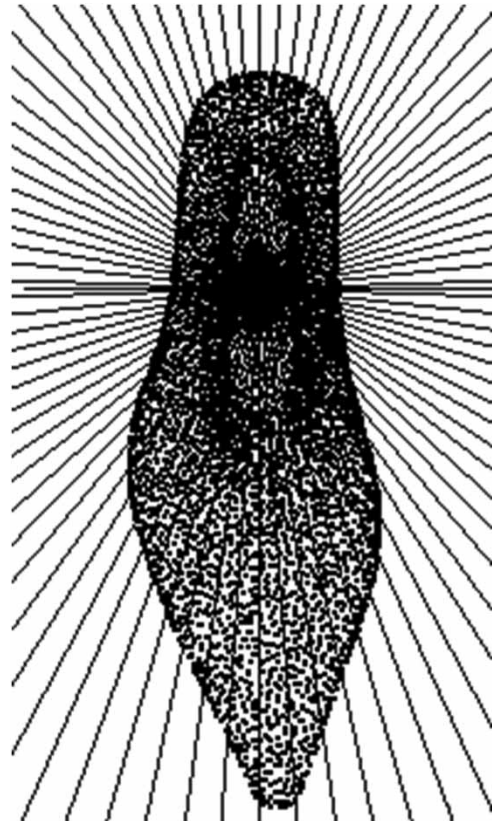


Fig. 15: Point cloud of shoe last model.

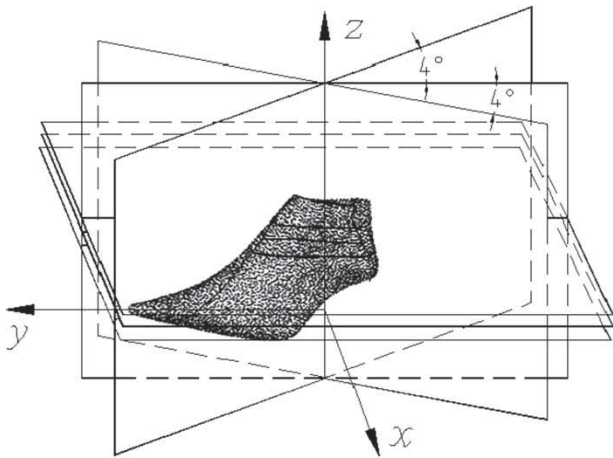


Fig. 16: Sketch of vertical planes for point cloud of shoe last model.

extrapolation method, according to the theory and computational steps of Section 3, to build the vertical projection planes, which will make 90 equal portions with the deviation angle $\theta = 4^\circ$ for the spatial point cloud (Fig. 16). Then, the point cloud on the vertical projection plane is searched and sorted, and an extrapolated curve (vertical contour curve) is reconstructed and total 90 points are obtained in each layer. Further, we use the IDS method to slice it and get a total of 183 layers (Fig. 17).



Fig. 17: Adaptive slice of shoe last point cloud using IDS method.

We obtain 90×183 intersection points through the intersection of obtained vertical contour curves and horizontal slicing plane. Then, the total of 90 points of an ordered contour on each layer is interpolated by using NURBS interpolation method and all interpolation curves are reconstructed. The two interpolation points in each interval $[u_i, u_{i+1}]$ are taken and 270 points in per layer are obtained. Fig. 18 illustrates the enlarged view of slicing contours of 120th, 121st and 122nd layers after the NURBS interpolation operation. Finally, by homogenizing the data points and

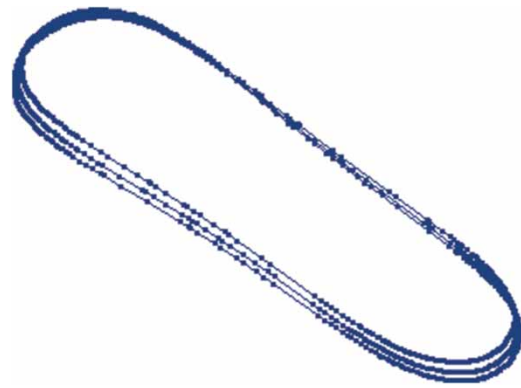


Fig. 18: Sliced contours after NURBS interpolation.

reducing their amount and taking 2° and 0.015 mm as the threshold of $\Delta\alpha$ and Δh respectively (Fig. 19), we can see that on the 121st layer there are total 87 data points.



Fig. 19: Data points on the 121st layer after points homogenizing and reducing.

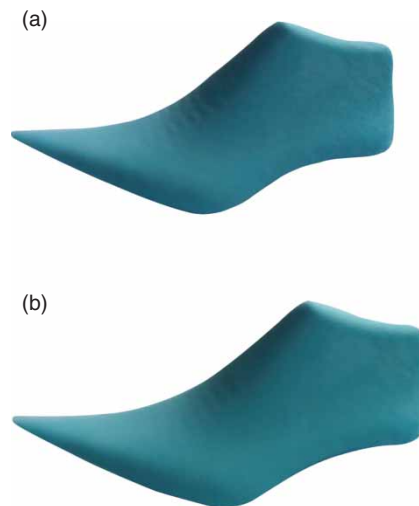


Fig. 20: Two rapid fabricating parts: (a) Rapid fabricating part, (b) Rapid fabricating part II.

The processed data of the shoe last with 183 layers is imported into the scanning path planning software for rapid prototyping and is fabricated into part I as shown in Fig. 20(a). We can see that the shoe last part

The point cloud division	Forming precision	Time cost for data processing	Time cost for RP
90 equal portions	0.013 mm	182 sec	780 min
180 equal portions	0.012 mm	205 sec	806 min

Tab. 2: Forming precision and processing speed of shoe last.

Errors between original part and final prototype	Length direction	Width direction	Height direction	Forming error
The absolute errors	0.012 mm	0.011 mm	0.012 mm	0.028 mm
The relative errors	0.04%	0.11%	0.08%	—

Tab. 3: Real error between original part and final prototype of shoe last.

is formed with a smooth surface and without distortion. For comparison, we also set $\theta = 2^\circ$ (180 equal portions) while building the vertical projection planes and obtain the rapid prototyping part II as shown in Fig. 20(b). Table 2 shows some related data of the two parts and there are no large differences in precision and time cost between the two rapid fabricating parts.

In order to demonstrate data processing precision of the algorithm in RE/RP integration system, the forming precisions of parts before scanning and after rapid fabricating are compared. Here the vertical slicing is undertaken with $\theta = 2^\circ$ (180 equal portions). Table 3 shows that the absolute errors and the relative errors in length, width and height direction and the forming error are all small. The rapid fabrication results meet the requirements of the forming precision.

9. CONCLUSION

This paper presents a series of novel slicing processing methods for spatial point cloud data based on the RE/RP integrated systems. Several simulation results and a shoe last practical example demonstrate that the methods take obvious advantages compared with the traditional methods because they avoid the complicated calculations such as searching associated points, solving intersections and calculating density of the spatial point cloud and that the methods reduce the time cost of data processing effectively. In addition, the presented algorithms can obtain the layered curve profile with high-precision and the data after homogenizing and reducing can be used directly for scan path planning. In RE/RP Integrated Manufacturing with spatial point cloud, using the series of algorithms presented in this study can maintain the original model feature shape and obtain higher forming precision. The deficiencies of this paper are that there is no case examination for point cloud containing three features of convex, concave and internal structures and only models with smooth surfaces are

discussed. Also, the compatibility problem of the processed data with other rapid prototyping machines needs to be further studied.

ACKNOWLEDGEMENTS

This work was supported by the National Natural Science Foundation of China (51075157); the Technology Development Project of Guangxi Education Department (201202ZD087); the Technology Development Project of Guangxi Science and Technology Department (No. 1010022-31); Program for Excellent Talents in Guangxi Higher Education Institutions.

REFERENCES

- [1] Yang, .P.; Qian, X.: Adaptive slicing of moving least squares surfaces: toward direct manufacturing of point set surfaces, *Computer Integrated Manufacturing Systems*, 8(3), 2008, 1-11. DOI: 10.1115/1.2955481.
- [2] Zhang, Y.F.; Wong, Y.S.; Loh, H.T.; Wu, Y.F.: An adaptive slicing approach to modeling cloud data for rapid prototyping, *Journal of Materials Processing Technology*, 140(1), 2003, 105-109. DOI: 10.1016/S0924-0136(03)00824-0.
- [3] Wu, Y.F.; Wong, Y.S.; Loh, H.T.; Zhang, Y.F.: Modeling cloud data using an adaptive slicing approach, *Computer-Aided Design*, 36(3), 2004, 231-240. DOI: 10.1016/S0010-4485(03)00097-6.
- [4] Lee, K.H.; Woo, H.: Direct integration of reverse engineering and rapid prototyping, *Computers & Industrial Engineering*, 38(1), 2000, 21-38. DOI: 10.1016/S0360-8352(00)00017-6.
- [5] Ren, N.F.; Hu, R.X.; Wan, J.: Study on adaptive point data slicing, *Transactions of the Chinese Society of Agricultural Machinery*, 37, 2006, 118-121. DOI: 10.3969/j.issn.1000-1298.2006.02.031.
- [6] Sun, Y.W.; Gu, Z.Y.; Wang, Y.C.: Rapid prototyping manufacturing based on cloud data

- from FREE-FORM surface, *Journal of Mechanical Engineering*, 39, 2003, 56-39. DOI: 10.3901/JME.2003.01.056.
- [7] Liu, G.H.; Wong, Y.S.; Zhang, Y.F.; Loh, H.T.: Error-based segmentation of cloud data for direct rapid prototyping, *Computer-Aided Design*, 35(7), 2003, 633-645. DOI: 10.1016/S0010-4485(02) 00087-8.
- [8] Levin, D.: The approximation power of moving least-squares, *Mathematics of computation*, 67(224), 1998, 1517-1531. DOI: 10.1090/S0025-5718-98-00974-0.
- [9] Milroy, M.; Bradley, C.; Vickers, G.: Segmentation of a wrap-around model using an active contour, *Computer-Aided Design*, 29(4), 1997, 299-320. DOI:10.1016/S0010-4485(96)00058-10.1007/s00170-004-2281-6.
- [10] Liu, Y.F.; Ke, Y.L.: Hybrid slicing technology in reverse engineering, *Journal of Computer-aided Design & Computer Graphics*, 15, 2003, 741-745. DOI:10.3321/j.issn:1003-9775.2003.06.020.
- [11] Goovaerts: Geostatistical approaches for incorporating elevation into the spatial interpolation of rainfall, *Journal of hydrology*, 228 (1), 2000, 113-129. DOI: 10.1016/S0022-1694(00) 00144-X.
- [12] Deng, J.Z.: *Extrapolation and its Application*, Shanghai Science and Technology Publications, Shanghai, 1984.
- [13] Shi, H.L.: *New ideas and methods of design errors*, Science Publications, Beijing, 2007.
- [14] Zimmerman, D.; Pavlik, C.; Ruggles, A.; Armstrong, M.: An experimental comparison of ordinary and universal kriging and inverse distance weighting, *Mathematical Geology*, 31(4), 1999, 375-390. DOI: 10.1023/A: 1007586507433.
- [15] Rogers, D.: *An introduction to NURBS: with historical perspective*, Morgan Kaufmann, Los Altos, 2001.
- [16] Shi, F.Z.: *CAGD&NURBS*, Beijing Aeronautics & Astronautics University Press, Beijing: 1994.
- [17] Sun, Y.W.; Dong, M.G.; Zhen, Y.J.: B-spline surface reconstruction and direct slicing from point cloud, *The International Journal of Advanced Manufacturing Technology*, 27, 2006, 918-924. DOI: 10.1007/s00170-004-2281-6
- [18] Lee, K.H.; Woo, H.; Suk, T.: Data reduction methods for reverse engineering, *The International Journal of Advanced Manufacturing Technology*, 17 (10), 2001, 735-43. DOI: 10.1007/s001700170119